JOURNAL OF CIVIL ENGINEERING AND MANAGEMENT
ISSN 1392-1541 print/ISSN 1822-3605 online
2011 Volume 17(1): 88–97
doi:10.3846/13923730.2011.556180

HEAT EXCHANGE IN THE SURFACE OF LIGHTWEIGHT STEEL ROOF COATINGS

Karolis Banionis[1], Vytautas Stankevičius[2], Edmundas Monstvilas[3]

Institute of Architecture and Construction of Kaunas University of Technology,
Tunelio g. 60, LT-44405 Kaunas, Lithuania
E-mails: [1]karolis_banionis@yahoo.com (corresponding author);
[2]v.stankevicius@ktu.lt; [3]asi_monstvilas@yahoo.com

Received 29 Dec. 2009; accepted 13 Jul. 2010

Abstract. Exterior and interior air temperatures are commonly used for calculating the rated thermal parameters of the roofs. However, the values of heat flows of the lightweight ventilated roofs are determined by the difference between the temperatures of premises and the ventilated air gap of the roof rather than by the difference between exterior and interior air temperatures. The temperature of the ventilated air gap of the roof is strongly influenced by the temperature of steel roof coating having low thermal receptivity, thus its temperature quickly reacts to solar radiation, long-wave radiation from the sky and other climatic effects. This paper presents the results of theoretical and experimental studies on heat exchange among external climate, roof coating and the ventilated air gap of lightweight roof, including regularities of variations in the temperatures of roof coating.

Keywords: lightweight steel roofs, solar radiation, short-wave radiation, long-wave radiation, ventilated air gap, temperature of roof coating.

1. Introduction

In the continental or colder climate regions, technical and thermal solutions of lightweight ventilated roofs are based on heat saving during the cold period of the year. During the process of roof design, the heat exchange processes which take place during the summer period are not considered. In summer the problem of overheated premises under the lightweight ventilated steel roofs is encountered: sun radiation heats the surfaces of the buildings and for this reason, the indoor temperature increases (Šeduikytė and Paukštys 2008). Moreover, the surface temperatures of the buildings can easily reach 75–80 °C (Lee *et al.* 2009). In summer steel roof coatings heat due to the intensive solar radiation and this causes additional heat gains in the premises. The calculation of values of the heat gains requires the following:

a) to estimate the temperature of the roof coating, i.e. to evaluate the heat exchange among the exterior, roof coating and ventilated air gap;
b) to estimate the temperature of the ventilated air gap, i.e. to evaluate the heat exchange among the roof coating, ventilated air gap and roof construction, which is situated between the ventilated air gap and premises;
c) to estimate the thermal behavior of the roof construction, situated between the ventilated air gap and premises, and the temperature differences between the ventilated air gap and premises, i.e. to evaluate the heat exchange between the ventilated air gap and premises through the roof construction.

Normally, the calculations of rated thermal parameters are carried out using the interior and exterior air temperatures. Heat flow values of lightweight ventilated steel roofs are determined by the temperature differences between the premises and ventilated air gap of the roof, but not by the temperature differences between the premises and exterior air. The temperature of the ventilated air gap of the roof is influenced by the temperature of steel roof coating. The coating has a low thermal receptivity, thus its temperature quickly reacts to the solar radiation, long-wave radiation from the sky and other climatic impacts. Daily variation of climatic impacts causes significant changes in the temperature of the steel roof coating. Therefore, thermal analysis of the roof is often time dependent since the external climate temperature, wind speed and solar radiation vary with time (Al-Sanea 2002). Similarly, the temperature distribution inside the multilayer lightweight partitions is effected not only by the temperature differences of both surfaces of the partition, but also by the direct solar radiation onto the external surface (Kairys *et al.* 2006).

Primary comparative calculations of steel and tiling roof coating parameters indicated that thermal diffusivity of steel coating is approximately $140 \cdot 10^{-7}$ m^2/s and of tilling coating approximately $6 \cdot 10^{-7}$ m^2/s, i.e. thermal diffusivity of the steel roof coating is 23 times higher than that of the tiling coating. Raising the steel coating temperature of 1 m^2 by one degree requires approximately 16 times less energy than the tiling coating. The calculation method of unsteady heat exchange employs the parameter of maximum time step (Barkauskas and

Copyright © 2011 Vilnius Gediminas Technical University (VGTU) Press Technika
www.informaworld.com/tcem

Stankevičius 2000). It indicates the amount of time needed for the heat exchange between the analyzed surfaces to become steady. In the case of the steel roof coating of 0.5 mm thickness, the allowable time step is approximately 0.009 seconds, whereas for tiling it is 0.2 seconds; thus, in tiling layer, the heat exchange becomes steady approximately 22 times slower. The results of the presented comparative calculations enable to make a presumption that the ventilated steel roof coating instantly reacts to the thermal effects of climate due to the rapid heat exchange processes.

Apart from the exterior air temperature, the temperature of roof coating is influenced by the short-wave and long-wave thermal radiation, the angle of the surface of the roof and the horizontal projection, and the short-wave absorption and long-wave absorption coefficients of the surface. Before calculating the external surface temperature, the heat exchange in the external surface of the roof coating should be estimated.

Thermal conductivity of the external surface of the roof coating is defined as the external heat transfer coefficient. The external heat transfer coefficient of roof coating is estimated from the constituent sum of convective and radiative heat transfer coefficients of the external surface (EN ISO 6946:2008; Oliveti *et al.* 2003; Al-Sanea 2003) (see Eq. 1):

$$h_{se} = h_r + h_c. \quad (1)$$

The radiative constituent of heat transfer coefficient of the exterior surface of the roof is calculated according to Eq. (2) (EN ISO 6946:2008, Biwole *et al.* 2008; Hadavand *et al.* 2008a; Hadavand *et al.* 2008b):

$$h_r = 4 \cdot \sigma \cdot T_{AIR}^3 \cdot (\frac{1}{\varepsilon_{sky}} + \frac{1}{\varepsilon_{surf}} - 1), \quad (2)$$

where: h_r – radiative heat transfer coefficient of the exterior surface of the roof, W/(m^2·K); σ – Stefan-Boltzmann constant, σ = 5.67051·10^{-8} W/(m^2·K^4); T_{AIR} – exterior air temperature, ºK; ε_{sky} – emissivity of long-wave radiation from the sky; ε_{surf} – emissivity of long-wave radiation of exterior surface of the roof.

The value of the convective heat transfer coefficient of the exterior surface of the roof is dependent on the wind speed v (m/s) (Фокин 2006) and is calculated according to the following Eq. (3.1):

$$h_c = 7.34 \cdot v^{0,656} + 3.78 \cdot e^{-1,91 \cdot v} \quad (3.1)$$

or given by Černe and Medved (2007):

$$h_c = 3.1 + 4.1 \cdot v. \quad (3.2)$$

Under solar radiation, the temperature of exterior surface of the envelope increases, whereas the effect of long-wave radiation from the sky reduces it. As it is described by (Шкловер *et al.* 1956), solar and long-wave radiations have an impact on the relative exterior air temperature. This temperature θ_{sol} (°C) is calculated by (Шкловер *et al.* 1956) as follows:

$$\theta_{sol} = \theta_e + \frac{\alpha_{surf} \cdot I_t}{h_{se}} - 3.6, \quad (4)$$

where: θ_e – average exterior air temperature, °C; I_t – intensity of solar radiation to the surface of adequate orientation, W/m^2; α_{surf} – surface short-wave absorption coefficient; h_{se} – heat transfer coefficient of the external surface, W/(m^2·K); $\frac{\alpha_{surf} \cdot I_t}{h_{se}}$ – equivalent temperature of solar radiation, °C; 3.6 – decrease of the average relative exterior air temperature due to the long-wave radiation.

The methodology for calculation of the surface temperature θ_{se} is described by Ulgen (2002) and Kaşka *et al.* (2009) where solar radiation and long-wave radiation from the sky, relative exterior air temperature, heat exchange in superficial layers and thermal energy absorption coefficients of surfaces are evaluated. The equation suggested by (Kaşka *et al.* 2009) is similar to the one proposed by (Шкловер *et al*. 1956) but there is one fundamental difference.

In contrast to (Шкловер *et al.* 1956 and Kaşka *et al.* 2009) it is stated that the impact of solar and long-wave radiation effect is attributed not to the relative exterior air temperature evaluation, but to the evaluation of temperature variation of the surface, affected by these radiations, as follows (ASHRAE 2001):

$$\theta_{se} = \theta_e + \frac{\alpha_{suf} \cdot I_t}{h_{se}} - \frac{\varepsilon_{surf} \cdot \Delta R}{h_{se}}, \quad (5)$$

where: ΔR – the balance of long-wave radiation (the long-wave radiation from the sky minus the long-wave radiation of the surface of the roof coating), W/m^2; $\frac{\varepsilon_{surf} \cdot \Delta R}{h_{se}}$ – amendment item for the evaluation of exchange between the long-wave radiation from the sky and the long-wave radiation of the surface of the roof coating.

In accordance with ASHRAE recommendations (ASHRAE 2001), this amendment item can be used as a constant and is 4 °C for horizontal surfaces, i.e. surface temperature declines by 4 °C due to the long-wave radiation effect. For vertical surfaces this amendment item is 0 °C (Ulgen 2002).

According to EN ISO 13790:2008 standard, horizontal surfaces fully take over the effects of long-wave radiation, but these effects are twice less for vertical surfaces. Kehrer and Schmidt (2008) provide an amendment for the estimation of long-wave radiation effect due to the surface lean angle. Thus, the external surface temperature of the ventilated lightweight steel roofs $\theta_{rc.e}$ should be calculated according to the following Eq. (6):

$$\theta_{rc.se} = \theta_e + \frac{I_{\Sigma.SOL} \cdot \alpha_{rc.se}}{h_{rc.se}} + \frac{\Delta L_{NET} \cdot \varepsilon_{rc.se}}{h_{rc.se}} \cdot (\cos(\frac{\beta}{2}))^2, \quad (6)$$

where: ΔL_{NET} – the balance of long-wave radiation (the long-wave radiation of the surface of the roof coating minus the long-wave radiation from the sky), W/m^2;

β – the angle of the relevant surface of the roof coating with the horizontal plane.

Together with the climatic thermal effects on the external surface of the roof coating, heat exchange takes place in the interior surface of the roof coating. The exchange affects the interior surface of the roof coating and for this reason, its evaluation is necessary for the analysis of the consistent patterns of temperature variations of the surface of the roof coating (Fig. 1).

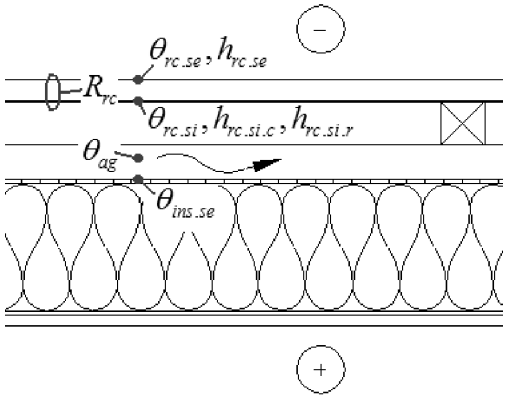

Fig. 1. Figures used for the calculation of heat exchange in the surfaces of the roof coating

For this purpose, the energy balance Eq. (7) could be used to calculate the temperature of the interior surface of the roof coating $\theta_{rc.si}$ in the following manner (8):

$$\frac{\theta_{rc.se}-\theta_{rc.si}}{R_{rc}} = (\theta_{rc.si}-\theta_{ag})\cdot h_{rc.si.c} + (\theta_{rc.si}-\theta_{ins.se})\cdot h_{rc.si.r}, \quad (7)$$

$$\theta_{rc.si} = \frac{h_{rc.si.c}\cdot R_{rc}\cdot\theta_{ag} + h_{rc.si.r}\cdot R_{rc}\cdot\theta_{ins.se} + \theta_{rc.se}}{h_{rc.si.c}\cdot R_{rc} + h_{rc.si.r}\cdot R_{rc} + 1}, \quad (8)$$

where: $\theta_{rc.si}$ – temperature of the interior surface of the roof coating, ºC; θ_{ag} – temperature of the ventilated air gap of the roof, ºC; $\theta_{ins.se}$ – temperature of the external surface of the roof thermal insulation layer, ºC; R_{rc} – thermal resistant of the roof coating, m^2·K/W; $h_{rc.si}$ – heat transfer coefficient of the interior surface of the roof coating, W/(m^2·K).

Heat exchange in the internal surface of the roof coating is divided into convective and radiative heat exchange. The former takes place between the internal surface of the roof coating and the air moving in the ventilated air gap, while the latter refers to the exchange through the ventilated air gap between its boundary surfaces, i.e. between the internal surface of the roof coating and the external surface of the roof thermal insulation layer. In Eqs. (7) and (8), the convective heat transfer coefficient of the internal surface of the roof coating $h_{rc.si.c}$ (W/(m^2·K)) is calculated by Eq. (3) where the speed of the air moving through the ventilated air gap is applied instead of the wind speed. The radiative coefficient of the same surface $h_{rc.si.r}$ (W/(m^2·K)) is calculated according to the following equation, provided by (Ong and Chow 2003; Barkauskas and Stankevičius 2000; Šadauskienė *et al.* 2009):

$$h_{rc.si.r} = \frac{\left(\frac{273+\theta_{rc.si}}{100}\right)^4 - \left(\frac{273+\theta_{ins.se}}{100}\right)^4}{\theta_{rc.si}-\theta_{ins.se}} \cdot \frac{C_o}{\frac{1}{\varepsilon_{rc.si}} + \frac{1}{\varepsilon_{ins.se}} - 1}, \quad (9)$$

where: C_o – radiation coefficient of black-body, C_o = 5.67 W/(m^2·K^4).

The value of the convective heat transfer coefficient depends on the speed of the air moving through the ventilated air gap, but the characteristics of roof construction below the air gap have no effect on its value. Moreover, following Eq. (9), the radiative heat transfer coefficient of the surface depends on the long-wave radiation emissivity of the boundary surfaces of the ventilated air gap and their temperature. The value of the radiative heat transfer coefficient can be increased and reduced by changing the long-wave radiation emissivity of these surfaces: reduced emissivity diminishes the value of the coefficient and vice versa. One of the solutions for reducing the radiative heat transfer through the ventilated air gap is to install a layer with low radiative emissivity in the lower surface of the gap. When the internal surface of the roof coating is $\varepsilon_{rc.si}$ = 0.8 and the lower surface of the ventilated air gap $\varepsilon_{ins.se}$ is reduced from 0.9 to 0.1, the value of the radiative heat transfer coefficient can be reduced about 7 times. However, in this case, a part of the radiative energy would be reflected from this layer and this amount of energy would increase the temperature of the interior surface of the roof coating, though it is still unknown how much this temperature could increase. In theory, according to Eq. (9), when the temperature of the interior surface of the roof coating $\theta_{ins.se}$ is reduced, the radiative heat transfer coefficient also decreases. This suggests that a thermally recipient layer, which would accumulate a part of thermal energy, installed in the lower surface of the ventilated air gap, or two gaps installed instead of one would give the reason for the temperature variation of the roof coating; however, this presumption has not been studied yet.

In order to investigate the processes and dynamics of heat exchange between the atmosphere and the surface of the ventilated lightweight steel roof coating, and to evaluate the reliability of the methodology for calculating the temperature of the coatings, the experiments were performed as described below.

2. Objectives of the experiments and construction of experimental cells

Commonly used constructions of lightweight ventilated roofs with steel coatings were chosen for experimentation. In such types of roofs, thermal insulation is usually installed between the wooden frame elements.

While planning the course of the experimentation, it was determined that the temperature of the ventilated steel roof coatings may be affected not only by the climatic impact, but also by the heat exchange between the coating and the external surface of the thermal insulation

layer of the roof. Aiming at the reduction of heat gains into the premises through the mentioned types of roofs during the hot season of the year, the external layers of thermal isolation of the roof could be equipped with heat reflective coatings, heat receptive layers made of constructional products, heat receptive layers with heat reflective coatings, or with more than one ventilated air gap.

The experiments were performed under real climatic conditions, which imply that the climatic effect was different for every experiment. If a single experimental cell had been used for the research, the comparison of the results, obtained at different times, would have been complicated. For this reason, two experimental cells of identical construction, S1 and S2 were prepared and their thermal characteristics were calibrated before the basic experimental stage. Having carried out the calibration of the cells (first experimental stage) and concluded that the thermal characteristics of the cells are identical, the construction of cell S1 was not altered during the whole experimental period. The construction of cell S2 was changed during the other experimental stages in order to estimate the impact caused by the thermal characteristics of roof layers, placed below the ventilated air gap, on the temperature variation dynamics of the roof coatings, arising due to the climatic effects. The experimental results of cell S2 were compared with those of cell S1.

Fig. 2 and Table 1 represents the roof construction of cells S1 and S2 during the first experimental stage (calibration of cells).

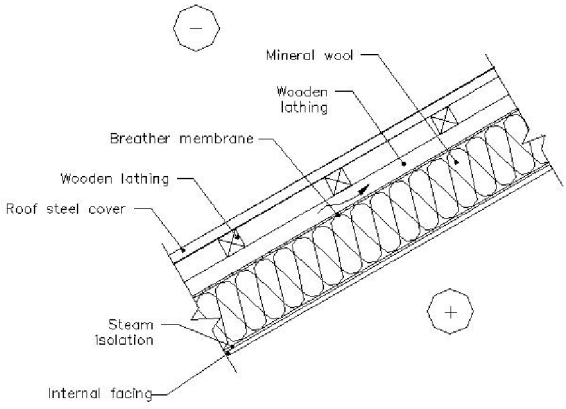

Fig. 2. The basic design of lightweight steel roof construction where a breather membrane is used for wind insulation

Table 1. Construction elements composing roof constructions of the cells

Material	Thickness, mm	Thermal conductivity, W/(m·K)
Roof steel cover	0.55	50
Breather membrane	0.6	0.13
Mineral wool	200	0.034
Polyethylene film	0.2	–*
Chipboard	10	0.13
Heat reflective film[1]	0.4	–*
Cement-sawdust board[2]	14	0.213

Note: [1] used in 2, 3, 5 experimental stages;
[2] used in 3, 4 experimental stages;
* R = 0.02 m²·K/W.

Heat transmittance coefficient of cells walls is U = 0.18 W/(m^2·K), cells floor U = 0.18 W/(m^2·K) and cells roof U = 0.16 W/(m^2·K). Profiled dark brown steel leafs were used as a waterproofing roof coating; their short-wave radiation emissivity of external surfaces is $\alpha_{rc.se}$ = 0.7, hemispherical long-wave radiation emissivity of external surfaces $\varepsilon_{rc.se}$ = 0.88 and hemispherical long-wave radiation emissivity of internal surfaces $\varepsilon_{rc.si}$ = 0.77 (Prado *et al.* 2005). A 0.6 mm thick breather membrane non-conductive for air functioned as a vapour-conductive wind proofing insulation (hereinafter "breather membrane"). Moreover, 10 mm thick chipboard was used for internal layer of roof construction. In order to maximally reduce the exterior air infiltration into the inside of the cells, the junctions of the premises and their separate layers were made airtight in both cells. Thermal insulation layers of walls and floor were made from 200 mm of expanded polystyrene foam panels. Two air conditioning devices of 400 W cooling capacities were also installed inside the cells. The orientation of roof surfaces of both cells was identical: south direction, whereas the surface lean angle towards the horizontal projection was 2°. The values of thermal conductivity coefficients of the constructional products used for the cells were evaluated by experimentations performed following LST EN 12667: 2002 and employing a device which meets ISO 8301:1991 requirements. The image of the cells is presented in Figs 3–7.

Fig. 3. Cells S1 and S2

The construction of cell S2 was changed in the other experimental stages as presented in Table 2.

In the roof constructions of the cells, the thermocouples were installed on the internal surface of the roof, in the middle of the ventilated air gap of the roof, on the external surface of the breather membrane, on the junction of the chipboard and polyethylene film, and on the internal surface of the chipboard. Additionally, two heat flux meters were installed on the internal surface of the roof of each cell. The internal temperature of the cells was measured by a digital meter TReg01, which was also used for its control, and a thermocouple T20. A digital meteorological station was set up near the cells for registering the exterior air temperature, diffuse solar radiation, total solar radiation, the balance of long-wave radiation, wind speed and other exterior air parameters.

Table 2. Roof construction of cell S2 in different experimental stages

Experiments	Changes of cell S2 construction in different experimental stages
2	A 0.3 mm thick heat reflective coating (Fig. 4) with a hemispherical long-wave radiation emissivity coefficient $\varepsilon_h = 0.09$ was mounted over the breather membrane.
3	A 14 mm thick cement-sawdust board ($\lambda = 0.213$ W/m·K) with heat reflective coating (Fig. 5) and a hemispherical long-wave radiation emissivity coefficient $\varepsilon_h = 0.09$ was mounted over the breather membrane. Heat capacity of the board per area is 26572 J/(m^2·K).
4	A 14 mm thick cement-sawdust board ($\lambda = 0{,}213$ W/m·K) without additional coatings (Fig. 6) was mounted over the breather membrane. Heat capacity of the board per area is 26572 J/(m^2·K).
5	Two air gaps, separated by a heat reflective coating with two heat reflecting surfaces (Fig. 7), were installed over the breather membrane. The hemispherical long-wave radiation emissivity coefficient of these surfaces of the coating is $\varepsilon_h = 0.09$. The height of the air gap between the breather membrane and heat reflective coating is 35 mm, whereas the height of the air gap between the heat reflective coating and roof coating is 40 mm.

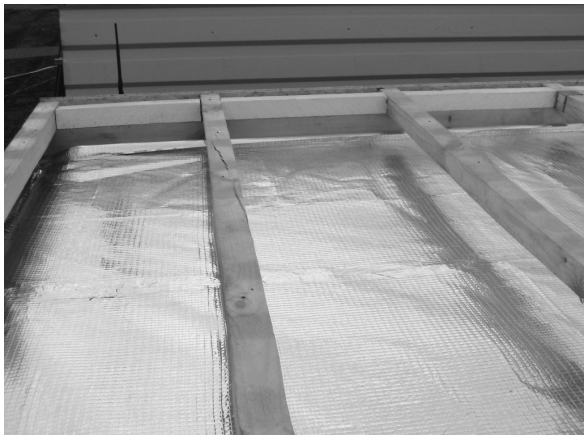

Fig. 4. The mounting of the heat reflective coating in cell S2 (exp. No. 2)

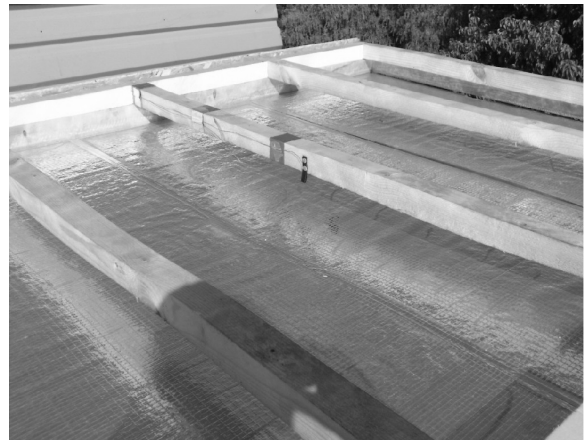

Fig. 5. The mounting of the cement-sawdust board with heat reflective coating in cell S2 (exp. No. 3)

Fig. 6. The mounting of the cement-sawdust board without additional coatings in cell S2 (exp. No. 4)

Fig. 7. The mounting of the two air gaps, separated by a heat reflective coating with two heat reflecting surfaces, in cell S2 (exp. No. 5)

During the experiments, a constant temperature of 10±0.5 °C which was lower than the exterior air temperature was maintained in the cells S1 and S2 all the time.

3. Meteorological data

The digital meteorological station, set up near the experimental roof cells, registered the following climatic parameters: diffuse and total solar radiation, long-wave radiation from the sky, exterior air temperature, relative humidity of the exterior air, wind speed, wind direction and atmospheric pressure.

The values of total solar radiation and balanced long-wave radiation, registered during the experiments, are presented in Figs 9, 10 and Table 3.

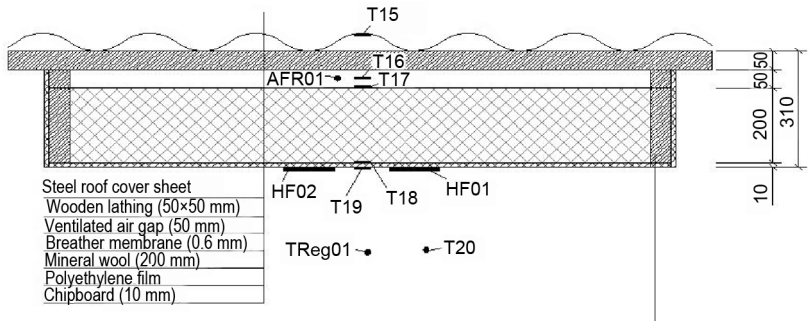

Fig. 8. The principle scheme of air flow, temperature and heat flux meter sensors arrangement in the roof construction, where: **T15** – Thermocouple on the interior surface of the roof coating;
T16 – Thermocouple in the middle of the ventilated air gap;
T17 – Thermocouple on the external surface of the breather membrane;
T18 – Thermocouple between the polyethylene film and chipboard;
T19 – Thermocouple on the interior surface of the chipboard;
T20 – Thermocouple inside the cell for measuring the internal temperature;
TReg01 – Digital temperature sensor inside the cell to measure and maintain the temperature;
HF01 – Heat flux meter on the interior surface of the chipboard;
HF02 – Heat flux meter on the interior surface of the chipboard;
AFR01 – Air flow sensor in the ventilated air gap of the roof

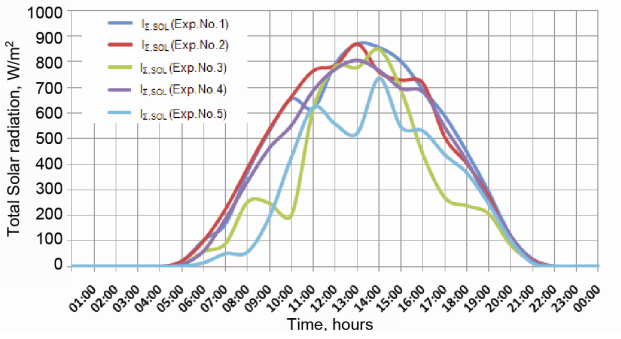

Fig. 9. Changes in the total solar radiation heat flow density in different experimental stages during 24 hours

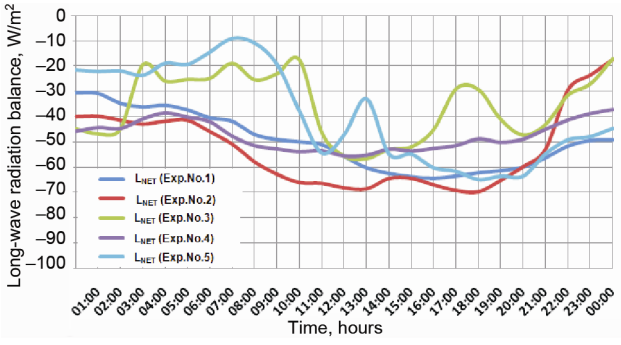

Fig. 10. Changes in the balanced long-wave radiation in different experimental stages during 24 hours

Table 3. Values and normative climatic data measured during the experiments of climatic parameters

Parameters	Exp. No. 1	Exp. No. 2	Exp. No. 3	Exp. No. 4	Exp. No. 5	Measured in July	Normative climatic data
Average daily exterior air temperature, °C	22.5	21.5	22.8	23.3	20.2	18.7	17.4
Average daily wind speed, m/s	2.3	1.2	1.8	1.9	1.3	1.7	3.1
Average daily total solar radiation, W/m²	331	327	242	307	225	222	215
Average daily diffuse solar radiation, W/m²	79	80	128	94	105	114	103
Average daily relative exterior air humidity, %	65	67	62	67	71	75	76
Average daily long-wave radiation from the sky to the top surface of the roof ↓, W/m²	388	385	404	394	388	382	n/a
Average daily long-wave radiation from the top surface of the roof to the sky ↑, W/m²	438	438	439	442	428	416	n/a
Average daily long-wave radiation balance, W/m²	–50	–53	–35	–48	–40	–34	n/a
Daylight period τ_d, hour.	17.4	17.2	16.9	16.7	16.0	16.6	16.0
Night time period τ_n, hour.	6.6	6.8	7.1	7.3	8.0	7.4	8.0

4. The experimental results

The experiments were carried out in Lithuania in the month of July because it has the highest average monthly air temperature. At this time, the average daily amplitude of the exterior air temperature is 10.2 °C and the maximum daily amplitude of the exterior air temperature is 18.7 °C (RSN 156-94). During the experimentation, the average daily amplitude of the exterior air temperature was 10.5 °C. Thus, it could be stated that the selected periods corresponded to the permanent monthly amplitude of the exterior air temperature in the experimental location (see Table 4).

Table 4. Measurement data of the exterior air and roof coating temperatures

Parameters	Cell No. 1 ("S1")			Cell No. 2 ("S2")		
	24 hours	Daylight hours	Night time hours	24 hours	Daylight hours	Night time hours
Experiment No. 1 (calibration of cells)						
Exterior air temperature, °C	22.5	23.5	20.0	22.5	23.5	20.0
Interior surface temperature of the roof coating, °C	29.9	34.8	17.0	29.7	34.6	17.0
Temperature difference between the interior surface of the roof coating and exterior air, °C	7.4	11.3	–3.0	7.2	11.1	–3.0
Experiment No. 2						
Exterior air temperature, °C	21.5	22.5	18.8	21.5	22.5	18.8
Interior surface temperature of the roof coating, °C	32.1	38.7	15.2	32.8	39.8	15.0
Temperature difference between the interior surface of the roof coating and exterior air, °C	10.6	16.2	–3.6	11.3	17.3	–3.8
Experiment No. 3						
Exterior air temperature, °C	22.8	24.0	20.1	22.8	24.0	20.1
Interior surface temperature of the roof coating, °C	28.7	33.7	16.9	29.7	35.2	16.8
Temperature difference between the interior surface of the roof coating and exterior air, °C	5.9	9.7	–3.2	6.9	11.2	–3.3
Experiment No. 4						
Exterior air temperature, °C	23.3	24.5	20.5	23.3	24.5	20.5
Interior surface temperature of the roof coating, °C	29.4	35.0	16.6	30.1	35.9	16.7
Temperature difference between the interior surface of the roof coating and exterior air, °C	6.1	10.5	–3.9	6.8	11.4	–3.8
Experiment No. 5						
Exterior air temperature, °C	20.2	20.8	19.0	20.2	20.8	19.0
Interior surface temperature of the roof coating, °C	27.9	34.0	15.8	28.5	35.3	15.1
Temperature difference between the interior surface of the roof coating and exterior air, °C	7.7	13.2	–3.2	8.3	14.5	–3.9

The results show that during the experimentation, the average daily temperature of the roof coating was higher, from 5.9–11.3 °C, than the exterior air temperature, while during the daylight hours, it was also higher, from 9.7 °C–17.3 °C. In the night time hours, the average temperature of the roof coating was lower, from 3.2 °C–3.9 °C, than the exterior air temperature, which was due to the long-wave radiation from the sky.

During the experiment No. 1, the difference between the average daily temperatures of the roof coating in the cells S1 and S2 was –0,2 °C, whereas during the experiments No. 2, No. 3, No. 4 and No. 5, these temperature differences were –0.7 °C, –1.0 °C, –0.7 °C and –0.6 °C respectively. This suggests that constructional changes of the roof, which theoretically should have an impact on the reduction of heat flows through the construction of the roof during the hot period of the day, increases the average daily temperature of the internal surface of the roof coating.

5. Experimental evaluation of theoretical presumptions

All data from the experimental cells and meteorological station were recorded every second; their average 1 minute value was calculated and stored in the data logging memory. Then they were transferred to the computer and processed by the Microsoft Excel. Tables 5 and 6 present the measured and calculated average hourly and daily results of roof coating temperatures and inaccuracies in their calculation.

Judging from the data, presented in Table 5, the absolute inaccuracy of the average hourly temperature of the interior surface of the roof coating, calculated by Eq. (8), is from –4.9 to +6.8 °C.

The data, presented in Table 6, suggests that the absolute inaccuracy of the average daily temperature of the roof coating, calculated by Eq. (8), is from –0.6 to +1.6 °C.

The calculations by Eq. (8) employed the experimental data on the temperature of the ventilated air gap, the speed of air moving in the ventilated air gap (for the evaluation of the convective heat exchange in the surface layers) and the temperature of the top surface of the thermal insulation layer of the roof. Then the results of the calculations by Eqs. (6) and (8) were compared in order to evaluate the impact of heat exchange intensity in the interior surface of the roof coating on the temperature of the coating. The heat exchange was determined to have the greatest impact when the temperature of the roof coating is the highest. However, the heat exchange reduces the temperature of the internal surface of the roof only approximately in 0.003 °C (the difference between the calculation results by Eqs. (6) and (8)). This implies that the radiative heat exchange between the surfaces of the ventilated air gap have no impact on the temperature of the ventilated steel roof coating; this type of coating takes over the thermal climatic effects in the extreme manner.

Table 5. Measured and calculated average hourly temperatures of the steel roof coatings of Cell No. 2

Time of the day	Exp. No. 1			Exp. No. 2			Exp. No. 3			Exp. No. 4			Exp. No. 5		
	M	*C*	*E*	*M*	*C*	*E*	*M*	*C*	*E*	*M*	*C*	*E*	*M*	*C*	*E*
00:00	18.0	18.8	0.8	12.9	14.5	1.6	11.8	14.4	–2.6	12.6	15.8	3.2	17.6	18.3	0.7
01:00	17,.7	18.4	0.7	12.9	14.7	1.8	13.2	15.2	–2.0	12.4	15.0	2.6	16.9	17.8	0.9
02:00	16.6	17.3	0.7	12.1	13.8	1.7	12.4	14.1	–1.7	13.7	15.2	1.5	15.9	17.2	1.3
03:00	15.7	16.6	0.9	13.4	13.6	0.2	14.6	16.0	–1.4	13.7	14.2	0.5	16.0	16.9	0.9
04:00	15.2	16.0	0.8	12.9	12.9	0.0	14.1	15.0	–0.9	13.6	13.8	0.2	15.9	16.5	0.6
05:00	15.4	16.6	1.2	13.3	13.6	0.3	15.0	15.8	–0.8	13.6	14.7	1.1	15.6	16.1	0.5
06:00	18.1	19.7	1.6	15.1	18.4	3.3	17.9	18.6	–0.7	14.8	17.8	3.0	16.4	16.6	0.2
07:00	21.1	22.5	1.4	19.6	26.4	6.8	20.6	21.0	–0.4	18.5	24.8	6.3	17.3	18.8	1.5
08:00	29.0	31.1	2.1	31.9	36.9	5.0	27.7	27.8	–0.1	27.4	31.7	4.3	18.0	19.2	1.2
09:00	36.1	38.1	2.0	44.8	46.7	1.9	28.4	28.4	0.0	34.6	37.3	2.7	25.8	23.9	–1.9
10:00	39.8	41.6	1.8	51.8	52.2	0.4	28.7	27.8	0.9	41.1	43.0	1.9	37.6	35.6	–2.0
11:00	40.0	41.6	1.6	56.7	56.4	–0.3	46.3	41.9	4.4	43.9	44.5	0.6	48.1	44.9	–3.2
12:00	46.4	47.6	1.2	58.4	58.3	–0.1	52.3	46.7	5.6	49.7	48.4	–1.3	46.4	41.5	–4.9
13:00	49.2	49.3	0,1	62.4	58.5	–3.9	51.6	47.7	3.9	50.1	48.9	–1.2	46.9	44.0	–2.9
14:00	51.0	51.5	0.5	57.6	55.2	–2.4	57.8	51.3	6.5	48.1	46.9	–1.2	56.3	53.0	–3.3
15:00	48.2	49.4	1.2	55.2	53.4	–1.8	49.3	46.6	2.7	48.6	46.0	–2.6	50.5	46.4	–4.1
16:00	44.9	46.4	1.5	53.6	50.6	–3.0	41.2	39.9	1.3	46.5	44.9	–1.6	48.9	44.1	–4.8
17:00	41.7	43.8	2.1	44.9	43.7	–1.2	36.5	36.0	0.5	43.3	42.7	–0.6	43.2	39.6	–3.6
18:00	36.0	38.8	2.8	40.5	40.6	0.1	36.7	36.0	0.7	38.5	38.8	0.3	39.0	37.0	–2.0
19:00	30.6	33.8	3.2	32.1	34.1	2.0	34.4	34.0	0.4	32.9	33.8	0,9	31.5	31.8	0.3
20:00	25.4	27.4	2.0	24.3	26.5	2.2	26.9	27.6	–0.7	28.3	29.3	1.0	22.6	24.6	2.0
21:00	21.5	22.9	1.4	20.0	22.0	2.0	22.6	23,8	–1.2	24.4	24.9	0.5	15.2	19.1	3.9
22:00	19.2	20.3	1.1	17.8	20.0	2.2	21.3	22.6	–1.3	22.0	23.1	1.1	15.0	18.1	3.1
23:00	18.2	19.3	1.1	17.4	19.9	2.5	21.4	22.6	–1.2	21.5	22.6	1.1	14.2	17.1	2.9
00:00	17.0	18.2	1.2	18.9	20.0	1.1	21.4	22.4	–1.0	21.2	21.9	0.7	11.7	15.7	4.0

***Note: M** – measured temperature, **C** – calculated temperature, **E** – absolute calculation error (the difference between the temperature of the interior surface of the roof, calculated by equation (7), and the measured temperature)*

Table 6. Measured and calculated average daily temperatures of the steel roof coatings

Parameters	Experiment No. 1		Experiment No. 2		Experiment No. 3		Experiment No. 4		Experiment No. 5	
	"S1"	"S2"	"S1"	"S2"	"S1"	"S2"	"S1"	"S2"	"S1"	"S2"
Measured daily average temperature of the interior surface of the roof, °C	29.9	29.7	32.1	32.8	28.7	29.7	29.4	30.1	27.9	28.5
Calculated daily average temperature of the exterior surface of the roof by equation (6), °C	31.2	31.2	33.7	33.7	29.1	29.1	31.0	31.0	28.1	28.1
Calculated daily average temperature of the interior surface of the roof by equation (7), °C	31.2	31.2	33.7	33.7	29.1	29.1	31.0	31.0	28.1	28.1
Absolute calculation error: the difference between the calculated temperature of the interior surface of the roof by equation (7) and the measured temperature, °C	1.3	1.5	1.6	0.9	0.4	–0.6	1.6	0.9	0.2	–0.4

***Note: "S1"** – Cell No. 1, **"S2"** – Cell No. 2.*

Thermal climatic effects on the steel roof coating can be divided into the following components of the temperature effects: exterior air temperature, the component of the short-wave solar radiation temperature and the component of the long-wave solar radiation temperature (Fig. 11).

During the experiment No. 3, the daily value variation of temperature components was calculated, using Eq. (6) and average hourly values of the climatic parameters, and presented in Fig. 12. It shows that the short-wave solar radiation and the exterior air temperature have the greatest effect on the temperature variation of the roof coating. Due to the thermal effects of the solar radiation, this experiment estimated the temperature of the coating up to 25 °C higher than the value of the exterior air temperature (Fig. 13, 14:00 h). During the experiment, the effect of long-wave solar radiation was minor and reduced the temperature of the coating only by approximately 1–4 °C.

$$\theta_{rc.se} = \theta_e + \frac{I_{\Sigma.SOL} \cdot \alpha_{rc.se}}{h_{rc.se}} + \frac{\Delta L_{NET} \cdot \varepsilon_{rc.se}}{h_{rc.se}} \cdot (\cos(\frac{\beta}{2}))^2$$

$$\theta_{rc.se} = \theta_e + \theta_{s.w.r} + \theta_{l.w.r}$$

Fig. 11. Temperature components,
where: $\theta_{rc.se}$ – temperature of the roof coating, ºC; θ_e – exterior air temperature, ºC; $\theta_{s.w.r.}$ – temperature variation of the roof coating due to the effect of short-wave solar radiation, ºC; $\theta_{l.w.r.}$ – temperature variation of the roof coating due to the effect long-wave solar radiation, ºC

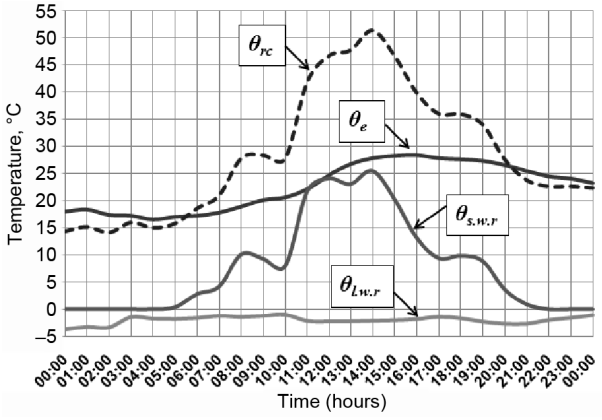

Fig. 12. Effect of the surface temperature of the roof coating on the daily value variation of the components. The results of calculation by equation (6) and average values of hourly climatic rates

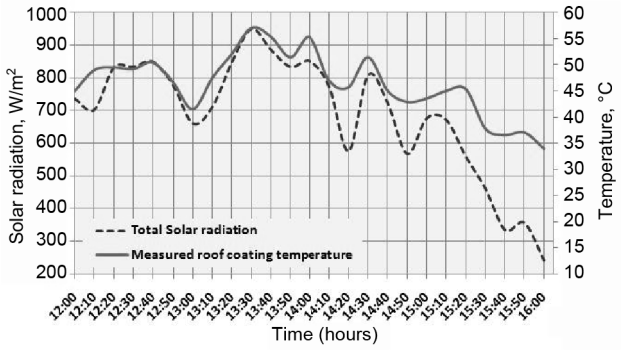

Fig. 13. Temperature of the interior surface of the roof and the intensity of shot-wave solar radiation during the experiment. No. 3. Average values of 10 minutes

The temperature components of long-wave solar radiation effect and exterior air vary quite equally during 24 hours (Fig. 13). Dynamic temperature variation of roof coating during 24 hours is determined by the intensity of solar radiation effect. In practice, it is important to evaluate the amount of time required by the temperature of the roof coating to react to the solar thermal effects. Fig. 13 presents the diagrams showing the temperature of the internal surface of the roof coating and total short-wave solar radiation during the experiment No. 3. The data suggest that due to the low thermal emissivity, steel roof coatings quickly react to the thermal effects of solar radiation and their temperature variation repeat the complexion of the solar radiation intensity variation. The data obtained from the other experiments are very similar to the ones presented in Fig. 13.

5. Conclusions

1. Steel roof coatings take over the effects of thermal solar radiation quickly due to the low thermal susceptibility of the steel roofs. The temperature variation of the coatings repeats the complexion of the solar radiation intensity variation.

2. Radiative heat exchange between the boundary surfaces of the ventilated air gap has almost no impact on the temperature of the ventilated steel roof coating. This type of coatings takes over thermal climatic effects in the extreme manner.

3. Calculation methodology was used for the estimation of the temperature of the ventilated steel roof coating. This methodology assesses long-wave radiation from the sky, solar radiation, exterior air temperature and heat exchange in the ventilated air gap, and enables a precise calculation of the surface temperatures of the coating. The absolute error of the calculation is from –0.6 °C to +1.6 °C.

4. Short-wave solar radiation and exterior air temperature have the major impact on the temperature variation of the roof coating during 24 hours. Long-wave radiation from the sky has a lesser effect on the temperature of the coating, reducing it to approximately 1–4 °C.

References

Al-Sanea, S. A. 2002. Thermal performance of building roof elements, *Building and Environment* 37(7): 665–675. doi:10.1016/S0360-1323(01)00077-4

Al-Sanea, S. A. 2003. Finite-volume thermal analysis of building roofs under two-dimensional periodic conditions, *Building and Environment* 38(8): 1039–1049. doi:10.1016/S0360-1323(03)00068-4

ASHRAE. Handbook of fundamentals. 2001. American Society of Heating, Refrigerating and Air-Conditioning Engineers. Atlanta, GA.

Barkauskas, V.; Stankevičius, V. 2000. *Pastatų atitvarų šiluminė fizika* [Building physics]. Kaunas: Technologija.

Biwole, P. H.; Woloszyn, M.; Pompeo, C. 2008. Heat transfers in a double-skin roof ventilated by natural convection in summer time, *Energy and Buildings* 40(8): 1487–1497. doi:10.1016/j.enbuild.2008.02.004

Černe, B.; Medved, S. 2007. Determination of transient two-dimensional heat transfer in ventilated lightweight low sloped roof using Fourier series, *Building and Environment* 42(6): 2279–2288. doi:10.1016/j.buildenv.2006.04.022

EN ISO 6946:2008 Building components and building elements. Thermal resistance and thermal transmittance. Calculation method. Brussel, 2008.

EN ISO 13790:2008 Energy performance of buildings – Calculation of energy use for space heating and cooling. Brussel, 2008.

Hadavand, M.; Yaghoubi, M.; Emdad, H. 2008a. Thermal analysis of vaulted roofs, *Energy and Buildings* 40(3): 265–275. doi:10.1016/j.enbuild.2007.02.024

Hadavand, M.; Yaghoubi, M. 2008b. Thermal behavior of curved roof buildings exposed to solar radiation and wind flow for various orientations, *Applied Energy* 85(8): 663–679. doi:10.1016/j.apenergy.2008.01.002

Kairys, L.; Stankevičius, V.; Karbauskaitė, J. 2006. Heat flux through the timber walls under summer climate conditions in Eastern Europe, *Journal of Civil Engineering and Management* 12(1): 77–82.

Kaşka, Ö.; Yumrutaş, R.; Arpa, O. 2009. Theoretical and experimental investigation of total equivalent temperature difference (TETD) values for building walls and flat roofs in Turkey, *Applied Energy* 86(5): 737–747. doi:10.1016/j.apenergy.2008.09.010

Kehrer, M.; Schmidt, T. 2008. Radiation effects on exterior surfaces, in *Proc. of the 8th Symposium on Building Physics in the Nordic Countries*: *Selected papers, vol. 1. June 16–18, 2008, Copenhagen, Denmark.* Copenhagen: Danish Society of Engineers, 207–212.

Lee, S.; Park, S. H.; Yeo, M. S.; Kim, K. W. 2009. An experimental study on airflow in the cavity of a ventilated roof, *Building and Environment* 44(7): 1431–1439. doi:10.1016/j.buildenv.2008.09.009

LST EN 12667:2002 Thermal performance of building materials and products – Determination of thermal resistance by means of guarded hot plate and heat flow meter methods – Products of high and medium thermal resistance. 2002.

Oliveti, G.; Arcuri, N.; Ruffolo, S. 2003. Experimental investigation on thermal radiation exchange of horizontal outdoor surfaces, *Building and Environment* 38(1): 83–89. doi:10.1016/S0360-1323(02)00010-0

Ong, K. S.; Chow, C. C. 2003. Performance of a solar chimney, *Solar Energy* 74(1): 1–17. doi:10.1016/S0038-092X(03)00114-2

Prado, R. T. A.; Ferreira, F. L. 2005. Measurement of albedo and analysis of its influence the surface temperature of building roof materials, *Energy and Buildings* 37(4): 295–300. doi:10.1016/j.enbuild.2004.03.009

RSN 156-94 *Statybinė klimatologija* [Building climatology]. Vilnius, 1995.

Šadauskienė, J.; Buska, A.; Burlingis, A.; Bliūdžius, R.; Gailius, A. 2009. The effect of vertical air gaps to thermal transmittance of horizontal thermal insulating layer, *Journal of Civil Engineering and Management* 15(3): 309–315. doi:10.3846/1392-3730.2009.15.309-315

Šeduikytė, L.; Paukštys, V. 2008. Evaluation of indoor environment conditions in offices located in buildings with large glazed areas, *Journal of Civil Engineering and Management* 14(1): 39–44. doi:10.3846/1392-3730.2008.14.39-44

Ulgen, K. 2002. Experimental and theoretical investigation of effects of wall's thermophysical properties on time lag and decrement factor, *Energy and Buildings* 34(3): 273–278. doi:10.1016/S0378-7788(01)00087-1

Фокин, К. Ф. 2006. *Строительная теплотехника ограждающих частей зданий* [Phokin, K. PH. Thermal physics of building partitions]. Москва: АВОК-ПРЕСС.

Шкловер, А. М.; Васильев, Б. Ф.; Ушков, Ф. В. 1956. *Основы строительной теплотехники жилых и общественных зданий* [Shklover, A. M.; Vasilev, B. Ph.; Ushkov, Ph. V. Essential thermal technology of residential and public buildings]. Москва.

ŠILUMOS MAINAI PLIENINIŲ VĖDINAMŲ STOGŲ DANGŲ PAVIRŠIUOSE

K. Banionis, V. Stankevičius, E. Monstvilas

Santrauka

Stogų projektiniams šiluminiams rodikliams skaičiuoti įprastai naudojamos išorės oro ir vidaus patalpų temperatūros. Tačiau šilumos srautų vertes lengvųjų konstrukcijų vėdinamuose stoguose lemia ne temperatūrų skirtumas tarp išorės oro ir patalpų, bet temperatūrų skirtumas tarp patalpų ir vėdinamo oro tarpo stoge. Stogo vėdinamo oro tarpo temperatūrai didelę įtaką daro skardinės stogo dangos temperatūra. Šios skardinės dangos šiluminis imlumas yra mažas, todėl jos temperatūra greitai sureaguoja į Saulės spinduliuotės, dangaus skliauto ilgabangės spinduliuotės ir kitus klimato poveikius. Straipsnyje pateikti teoriniai ir eksperimentiniai šilumos mainų tarp išorės, stogo dangos ir vėdinamo oro tarpo lengvųjų konstrukcijų vėdinamuose stoguose tyrimų rezultatai ir stogo dangų temperatūros kitimo dėsningumai.

Reikšminiai žodžiai: lengvųjų konstrukcijų plieniniai stogai, Saulės spinduliuotė, trumpabangė spinduliuotė, ilgabangė spinduliuotė, vėdinamieji oro tarpai, stogo dangos temperatūra.

Karolis BANIONIS. PhD student of Civil Engineering, Researcher at the Laboratory of Thermal Building Physics of the institute of Architecture and Construction, KTU. Research interests: heat transfer, thermal impacts of solar radiation.

Vytautas STANKEVIČIUS. Doctor Habil, Full Professor, Chief Researcher at the Laboratory of Thermal Building Physics of the institute of Architecture and Construction, KTU. Research interests: heat transfer, technical properties of thermal insulation products.

Edmundas MONSTVILAS. Doctor, Senior Researcher at the Laboratory of Thermal Building Physics of the institute of Architecture and Construction, KTU. Research interests: heat transfer and thermal insulation, technical properties of thermal insulation products.